Nano World Journal

https://doi.org/10.17756/nwj.2023-s3-171

Research Article

Open Access

Machine Learning for Improved Nanomaterial Applications in Biology and Medicine: A Catalytic Perspective

Pramod Sridhara[1], Luis Buenaño[2], Sayuri Bonilla[2], Freddy Ajila[3], Rolando Marcel Torres Castillo[4], Mahaboob Khan Sulaiman[5] and Mayakannan Selvaraju[6*]

[1]*Department of Mathematics, Nitte Meenakshi Institute of Technology, Yelahanka, Bangalore, India*

[2]*Department of Mechanical Engineering, Escuela Superior Politécnica de Chimborazo (ESPOCH), Riobamba, Ecuador*

[3]*Facultad de Informática y Electrónica, Escuela Superior Politécnica de Chimborazo (ESPOCH), Sede Orellana, El Coca, Ecuador*

[4]*Department of Information Technology, Escuela Superior Politécnica de Chimborazo (ESPOCH), Riobamba, Ecuador*

[5]*Department of GRU Biologys, Fatima College of Health Sciences, Ajman, UAE*

[6]*Department of Mechanical Engineering, Vidyaa Vikas College of Engineering and Technology, Tiruchengode, Namakkal, Tamil Nadu, India*

***Correspondence to:**
Mayakannan Selvaraju
Department of Mechanical Engineering,
Vidyaa Vikas College of Engineering and Technology,
Tiruchengode, Namakkal, Tamil Nadu, India.
E-mail: kannanarchieves@gmail.com

Received: July 31, 2023
Accepted: November 01, 2023
Published: November 03, 2023

Citation: Sridhara P, Buenaño L, Bonilla S, Ajila F, Castillo RMT, et al. 2023. Machine Learning for Improved Nanomaterial Applications in Biology and Medicine: A Catalytic Perspective. *Nano World J* 9(S3): S966-S972.

Published by United Scientific Group

Abstract

Nanotechnology is the study of materials whose structures are between 0.1 and 100 nanometers in size, and their applications. The size effect, surface effect, and other unique characteristics of this material mean that it has a wide range of potential uses beyond those of more conventional materials. The increasing usage of nanoparticles in today's industries and lifestyles has sparked growing concern, particularly in the fields of biology and medicine. Researchers are now focusing on how to create multifunctional nanomaterials with features like magnetism and catalytic capabilities, and how to apply these materials more effectively in the field of biology. In addition to enhancing the quality of the wood, automatic detection of subpar wood is possible due to machine learning, which eliminates the possibility of human error due to eye tiredness or other subjective elements in the manual identification process. A measure of frequency of use. In this research, we focus on the application of the fuzzy analytic hierarchy approach to the investigation of nanocomposites and their catalytic performance in the oxidation of glucose. When comparing Ni_3S_2/IL-GR/GCE to glassy carbon bare electrode (GCE) and IL-GR/GCE, the latter has demonstrated much greater electrocatalytic activity for glucose oxidation. Using a sensitivity of S/N = 4, the linear range is from 0 to 1000 μm, and the detection limit is 0.162 μm. Ni_3S_2/IL-GR/GCE was shown to have a high level of anti-interference since the glucose current response was not considerably altered.

Keywords

Machine learning, Data processing, Nanomaterials technology, Fuzzy, Cluster analysis, Size effect

Introduction

Ship technology has been in a state of intense rivalry with other industries in recent years due to the rapid pace of industrial technological advancement. With the market how it is, huge corporations have no choice but to keep looking for new ways to get an edge [1]. In their pursuit of a breakthrough, they have prioritized three factors: low cost, high quality, and great efficiency. Recently implemented alternative techniques of producing heat include laser heating and electronic heating. They are more expensive but offer several benefits including ease of use, assurance of quality, and high productivity. In the first stages of development, more money will be spent because they will need to acquire expensive professional equipment. The basic idea behind heating of laser is to

constantly expose the metal plate to the heat of the laser beam. When compared to conventional heating methods, its pace is hundreds of times quicker, and it is easier to regulate, making it a great asset to automatic processing [2]. While heating, the metal plate's surface is protected from oxidation thanks to the use of the protective gas.

This study delves into various aspects of surface quality in machined surfaces, including precision maintenance, service life, corrosion resistance, and anti-stick properties [3]. The primary objective is to assess recent advancements in autonomous machining research involving nanomaterials. One notable development involves the fusion of pulse electrochemistry with an electrochemical mechanical finishing mechanism, resulting in a novel method for polishing mirrors in large reactors.

Furthermore, chochia's investigation focuses on the processing and automated analysis of video data obtained from a computer capillary mirror. This process includes addressing issues such as frame drift reduction and the generation of an averaged image from the original video data [4]. Key steps involve forming and sieving a contour map, analyzing the syntax of the contour, selecting the primary capillary, and preparing and analyzing the morphological characteristics of the contour. It is proposed to map the capillary region to the rectangular region using a homeomorphic alignment. The transformed information was used to characterize capillary blood flow. We present a method for tracking the time- and location-dependent variations in capillary blood flow velocity [5].

Within this analytical framework, the assessment of the failure of local bonds and flawed graphene within an ideal monolayer is based on the overall energy balance in the two-dimensional system [6]. Various mechanical parameters specific to the two-dimensional context, including Young's modulus, fracture strength, fracture toughness, line (edge) energy, and critical strain energy release rate, can be determined using a combination of experimental methods, density functional theory (DFT) calculations, molecular dynamics simulations, and a continuous two-dimensional model [7]. Remarkably, when observing the range from sub-nano meter to micro scales, the grave crack stress demonstrates a linear growth pattern relative to the square root of the effective defect length. It's worth noting that nanoscale imperfections like vacancies, cracks, and pre-cracks have minimal to no impact on the minimal limits of toughness of fracture and strain energy releasing rate [8]. When it comes to insulation failures in the electrical grid, the power tree is responsible, according to Pallon. Understanding the formation of the transmission tree is crucial for designing a robust HVDC system capable of transmitting voltages of up to 1.5 mV.

Perspective imaging with X-rays allows us to gain the capability to observe the electron tree within a cross-section of LDPE material in three dimensions, achieving an impressive resolution of 92 nm. In this three-dimensional perspective, the primary branches of the electronic tree become apparent, encased within a thin and broad front layer characterized by low density [9, 10]. Notably, proof that the tree expands gradually via the initial structure developed in front of the principal channel may be found in the form of a link between the pre-channel structure and the primary tree section, established through the material with lower density. It's worth emphasizing that none of these pre-channel structures surpass the threshold specified by Paschen's law, signifying that they are all too diminutive to evolve through partial discharge [11].

This study contributes to our knowledge by evaluating the geometry and scoring scheme of the component's casing. By gaining a deep understanding of the machining process, the research involves experimental analysis of surfaces produced through various methods like grinding and electrochemical machining. The friction and wear factors, the initial wear and accuracy preservation, the friction coefficients, and the component surface fatigue are all investigated. The insights gained from this comprehensive analysis of mechanical equipment performance, as outlined in reference [12], offer valuable technological guidance for enhancing the performance of diverse mechanical equipment components across various applications and advancing processing techniques. These features encompass durability, longevity, resistance to corrosion, and prevention of adhesion issues.

Nanomaterials Processing Automation Technology

Analysis of cluster

Machine learning is commonly categorized into two main types: supervised and unsupervised learning, depending on the presence or absence of prior information [13, 14]. Clustering is a prime example of unsupervised classification within the field of machine learning. Cluster analysis relies on analogies to gauge the level of similarity among objects, essentially grouping together those that exhibit strong connections while separating those with weaker connections [15-17].

Current non-conforming wood detecting technology is quite primitive when compared to other prosperous countries. The government has spent a lot of money on people and stuff because of the expensive detection equipment and the severe criteria of detection work in the workplace [18]. The process of looking for timber is entirely manual. Machine learning may identify the non-conforming timber, increasing wood use and reducing costs. This is because it eliminates the subjective elements that might impede human identification. Of course, there is room for improvement in machine learning's accuracy as well [17]. Various systems of classification establish a wide variety of electrochemical sensor types. In terms of the electrical signals, they produce, potential sensors, which measure changes in EMF, current sensors, which measure changes in current, and resistance sensors, which measure changes in resistance, may all be distinguished from one another [19]. DNA and enzyme sensors, non-biological ion sensors that use solid films, liquid models, and ion choices to detect ion categories, gas sensors that use semiconductors, combustion types, electrolysis, etc. to detect potentially dangerous gases like combustibles and explosives, etc. (Figure 1) [20].

Most clustering and grouping methods go through a series of standard steps, including data cleaning, feature selection

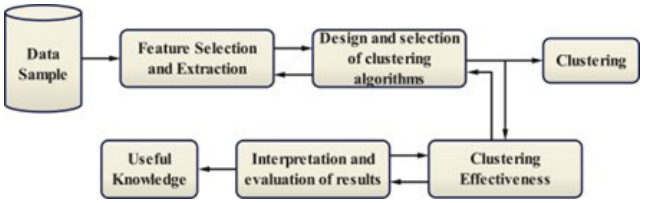

Figure 1: An outline of the clustering process.

or extraction, algorithm design, performance testing, result interpretation, and result evaluation [21].

The following calculation is performed under the assumption that there are m variables in the clustering data set.

$$X = \begin{bmatrix} X_{11} & X_{12} & \cdots & X_{1m} \\ X_{21} & X_{22} & \cdots & X_{2m} \\ \cdots & \cdots & \cdots & \cdots \\ X_{n1} & X_{n2} & \cdots & X_{nm} \end{bmatrix} \quad (1)$$

$$x_i = (x_{i1}, x_{i2}, \ldots, x_{im})^T \quad (2)$$

Clustering algorithms come in numerous forms, each catering to a unique set of data types and criteria for organizing information. Currently, the following are the most popular [22]

Grid: It mandates the use of the grid for all collective processing (cell). The grid method's complexity remains constant and is not influenced by the number of data sets, making it a suitable choice for data processing even when dealing with a large and diverse set of data points.

A distribution: Choose a suitable number of groups for your dataset of N data items, and classify each object completely into category K. The criteria for this approach is that items in one group have similar or identical characteristics, whereas items in another category have contrasting but irrelevant characteristics.

Density: The density-based clustering method overcomes the limitation that other algorithms can only handle spherical cluster data. It's applicable to any kind of cluster analysis. This technique is used to achieve the clustering goal by separating high-density from low-density areas.

A hierarchical approach: In contrast to the unified one-way aggregation of the partition technique, the data is divided into many layers of data sets before being aggregated in a hierarchical fashion. There are two types of algorithms for the cascade level: those that converge and those that diverge. Slow accumulation at the bottom characterizes the convergence process, whereas slow dispersal at the top defines the divergence process. In the cohesiveness algorithm, each data record is considered a separate group, and any two neighboring groups that merge into one another give rise to a new group [23].

Impact of size

The unique characteristics of nanoparticles, known as the "nanomaterial effect," include the following.

Quantum tunneling effect: The "potential barrier" phenomena will manifest itself in such tiny particles because of their distinct wave dimension, and this is something that cannot be described by classical physics [24].

Small scale effect: Once the material expands to the scale of several or even dozens of arranged atoms, its optical and electromagnetic properties become unique from those of the macromaterial. At this stage, the magnetic field rather than gravity determines the material's behaviour.

Surface effect: The small size and high specific surface area of this material result in a significant exposure of numerous active molecules on its surface. Furthermore, many of these molecules possess unsaturated chemical bonds, making it a strong contender for showcasing distinctive characteristics and capabilities.

Framework of organometallics

In anodizing, metals or alloys are oxidized electrochemically. When a metal or alloy is subjected to electrolysis and an electric current, an oxide layer develops on its surface. It is well-known that the anodizing temperature influences the nanotubes' diameter, thickness, and length. Tube elongation in aqueous solutions is inhibited by high temperatures, which speed up ion exchange and cause the collapse of the tube wall. However, the length of nanotubes will vary as a function of the organic electrolyte temperature [25]. When the nanotube cell is heated, ions diffuse more quickly. The breakdown of the basic barrier layer allows for the sustained growth of nanotubes because it creates a thin barrier layer with high mobility. Anodizing time has a significant impact on nanotube length, but it also has varying impacts on different electrolytes [26]. With hydrolysis, tube lengths remain constant because the anodizing process and the chemical corrosion response tend to balance out. Because the anodizing rate in organic electrolytes is always higher than the chemical corrosion rate, nanotube lengths remain reasonably steady over several days.

Porous materials excel in gas absorption and separation. The extent to which the stability of a bioactive group is impacted by the presence of a pore. Bond lengths formed by organic molecules are limited by the pore size of the residual material after macromolecules are removed [27]. Various biological adhesives can hold together substances with a wide range of moisture levels. MOFs are often employed for gas absorption and distribution when they have a small particle size and a high porosity. Drug binding and visual effects can be used to differentiate between the various methods of protein or peptide absorption and separation [28].

Fuzzy analytical hierarchy process (AHP)

Fuzzy AHP uses the following steps to evaluate potential schemes:

Step 1: Establish the index of assessment and the group of objects to be evaluated. Four criteria were used to assess the proposed scheme: dependability, cost, complexity, and production efficiency. To be reliable, a model must be able to perform as expected under specified conditions and during a certain time range; the cost index provides a ballpark figure for how much money will be spent on the

machinery over the course of its useful lifetime. , from initial development to decommissioning; and the complexity of the machine's structure reveals whether it makes use of cutting-edge technology to realize its optimal design. A machine's productivity is quantified by the number of jobs it can do in each production cycle, and its component assembly is simple and quick to operate.

Step 2: Create a framework using AHP. The ideal handle-producing mechanism candidate scheme may be thought of as the top layer of the model, while the criteria layer is represented by the factors in the evaluation index set.

Step 3: create an E-matrix of evaluations. The matrix E used in the evaluation may be written as:

$$E = \{P_1, P_2, P_3, P_4\} = \begin{bmatrix} r_{11} & r_{12} & r_{13} & r_{14} \\ r_{21} & r_{22} & r_{23} & r_{24} \\ \cdots & \cdots & \cdots & \cdots \\ r_{n1} & r_{n2} & r_{n3} & r_{n4} \end{bmatrix} \quad (3)$$

Before the evaluation matrix e can be computed, the evaluation object's priority vectors P1 through P4 must be specified.

Step 4: The evaluation's weight vector, w, must be calculated. Because the relative importance of different evaluation indices is a matter of opinion, F-AHP analysis requires that the relative weight of evaluation indices be provided. Like the preceding priority vector, the evaluation index weight vector is derived.

Step 5: Pick the best strategy by calculating the decision vector B. After assigning a weight vector to each cell of the evaluation matrix, we have the following decision vector B:

$$B = EW = (b_1, b_2, \ldots . b_n)^T \quad (4)$$

Experiment on the Automatic Processing

Process

Preparation

In this article, various analytical techniques were employed, including nitrogen adsorption instrument, X-ray powder diffraction (XRD), electron paramagnetic resonance (EPR), photoluminescence (PL), X-ray photoelectron spectroscopy (XPS), ultraviolet-visible absorption spectrum (UV VIS), and gas chromatography.

The CdTe quantum dots (QDs) were made by following a set protocol. The initial step was to combine several ingredients in a conical flask under nitrogen protection: 3 mL of 0.03 mol/l CdCl2 solution, 25 mM of trisodium zirconate dihydrate, 1.5 ml of fresh 0.01 mol/l sodium telluride, 65 mL of succinic acid, and 65 mL of sodium borohydride. Hydrothermal treatment of the combination for 50 min at 200 °C yielded a green solution and mercaptosuccinic acid-coated CdTe QDs in the orange colour. After being centrifuged at 5000 rpm, these CdTe QDs were washed in an ethanol solution of about 75%. After being dried under vacuum, the QDs were mixed with a 0.02 mol/l phosphoric acid buffer solution at pH 7.3 to create an optically clear sol.

Characterization of multilayers

Quantum dots may have an influence on bacterial activity if their surface potential is measured, their emission surface spectra are analysed, and they are distributed uniformly over multilayer surfaces.

Self-assembly of multilayer

Subsequently being submerged for 20 min in a 2 mg/ml PLL, PLL is then rinsed and dried in nitrogen. After soaking PLL for 30 min in CdTe dosage solution, the liquid is rinsed and dried in nitrogen to form a double-layer membrane in cdteqds/PLL.

Biological evaluation of antibacterial activity

In this study, two types of glass surfaces were employed: untreated glass and glass coated with ten layers of CdTe QDs/PLL films. These surfaces were used to disperse *E. coli* bacteria for analysis. The glass substrates were prepared by fixing them with 5% formaldehyde and dehydrating them using a stepwise ethanol gradient over a 2 h period at 37 °C. *E. coli* cultures were then introduced into LB medium that had been in contact with the glass media containing varying layers (ranging from 0 to 10) of CdTe QDs/PLL coatings. After allowing the *E. coli* cultures to grow for 12 h at 37 °C, their viability was monitored every two hours using a UV-visible absorption spectrophotometer set at 500 nm. This approach enabled the assessment of *E. coli* viability under different coating conditions.

Results and Discussion

Analysis of model optimization

To ensure that the constructed motor model properly simulates the operation of the actual motor, it is then subjected to a battery of tests on the motor test bench to determine how well the motor performs under a certain set of conditions. Motors are put through their paces on a specialized test bench in the first group, while models of motors are tested before and after optimization using hardware-in-the-loop in the second and third groups. The following are the findings obtained by gradually raising the required torque from 9 nm to 101 nm at 3500 r/min, 6500 r/min, and 9500 r/min while keeping an eye on the U-phase present factor in the motor control. A reading of the amplitude is taken. The three experimental groups' U-phase current amplitudes are displayed in figure 2, figure 3, and figure 4.

The close alignment between the results produced by the system and those from the actual motor serves as strong evidence of the system's accuracy. Furthermore, when the motor model accounts for losses and variable inductance characteristics, the error remains under 5%, well within the acceptable range for engineering applications. Enhancing the model with electrical induction parameters in real time, possibly as part of a data query or estimation system, can further boost accuracy and reduce wastage by improving hardware precision. To establish a dependable automatic test system for the PMSM controller, precise hardware in the loop is essential. The completion of this integrated test system involves refining the test process,

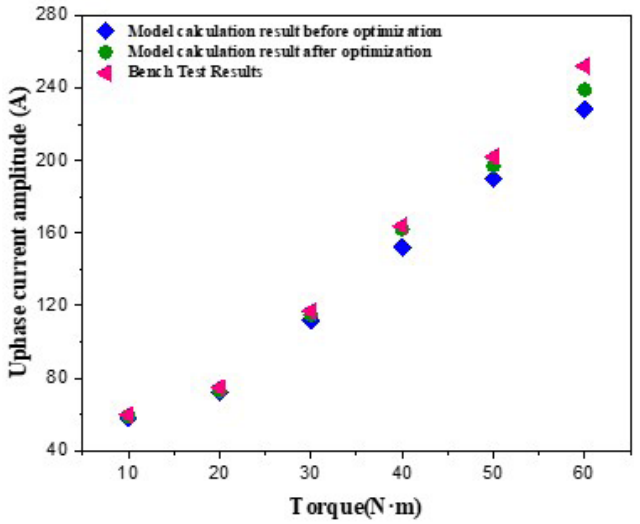

Figure 2: Amplitude of the U-phase current at 3500 rpm.

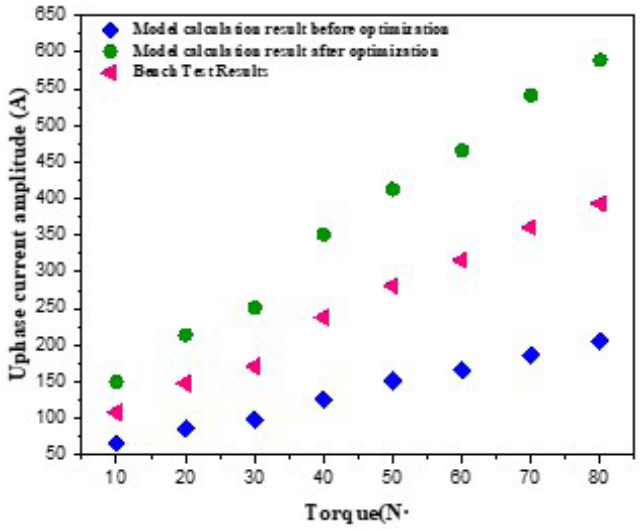

Figure 3: U-Amplitude of the U-phase current at 6500 rpm.

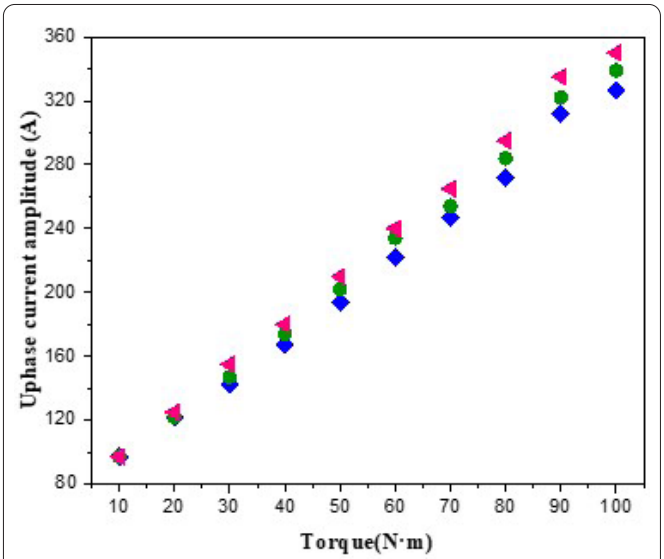

Figure 4: Amplitude of the U-phase current at 9500 rpm.

developing test management software, preparing test cases, and creating a comprehensive instrument. The functional test system requires both hardware and software to be created and built, with particular focus on the PXI real-time simulation system, the general signal conditioning unit, the defect entry unit, and the power management module. When the indicator, information, alarm, and display functions are thoroughly evaluated and a thorough test report is generated, we may say that the function test has been successful.

Nanosheet graphene oxide (GO): characterization and analysis

This work presents experimental results comparing the stability of three different sized GO suspensions at different pH levels, as measured by their zeta potentials. Table 1 shows that between the pH values of 4 and 10, GO-3 has the greatest negative zeta potential, with a zeta potential of less than 30 mv, whereas GO-1 reunites at a pH value of 1 to 4. In this configuration, the zeta potential cannot be measured. These results indicate that GO-3 colloid has more stability than GO-1 and GO-2.

Cellular absorption of graphene oxide nanosheets is greater than that of CNT, as seen in table 2. Cells from the experimental group were counted, and the absolute amount of material absorption was determined (in ng per 1000 cells).

Analysis on electrolytic conduction

Electrochemical mechanical finishing employs the anode in a non-linear electrolyte for several reasons. This choice results in a lower processing voltage, weaker electrochemical dissolution, and minimal gas production. However, the cathode's activation and passivation dissolving properties in a linear electrolyte are essential to electrochemical machining. Therefore, when the design of the tool head construction effectively manages exhaust, the impact of gas bubbles on conductivity can be disregarded. Currently, electrolyte conductivity is primarily influenced by electrolyte concentration and temperature. To address the potential issue of having an excessively large feature set from a single

Table 1: Three distinct GO suspensions, and their zeta potentials at varying pH levels.

PH	GO-1	GO-2	GO-3
4	-	-21.9	-36.4
6	-27	-34.6	-41.9
8	-31.6	-40.1	-45.2
10	-35.7	-41.2	-47.9

Table 2: Absorption of various nanomaterials by cells at various times.

Incubation time materials	2 h		24 h	
	Percentage	ng/10000 cell	Percentage	ng/10000 cell
GO1	3.61%	36.8	8.96%	331.4
GO2	6.23%	62.3	12.25%	428.8
GO3	9.12%	91.2	16.12%	602.3
SWNT	1.56%	15.6	9.54%	343.7
MWNT	5.14%	51.4	7.99%	282.9

scan image, the enhanced AP algorithm adopts a multi-scan approach, automatically adjusting the size of the sliding pane between scans for improved performance. This allows the data set's entry count to be decreased after feature extraction with each scan, boosting the algorithm's clustering efficiency and accuracy. Color moment, a method for extracting colour features, is used to get the data set that is then used in a SOM clustering algorithm to detect wood defects. K-means testing differentiates the SOM's clustering effect.

The conductivity of a solution is sensitive to its concentration and temperature because these factors affect the total amount of ions in the solution and the rate at which they flow. Concentration and temperature will affect the range across which the resistivity q can vary. The conductivity will be affected by both concentration and temperature, with the former having a more pronounced effect: at low concentrations, the range of resistivity change is restricted, but at high concentrations, the range is considerable.

An evaluation of production efficiency of photocatalytic hydrogen

The performance of pure TiO_2, pure Cu_2O, TiO_2 Ag, and TiO_2 Ag@Cu_2O materials in photocatalytic hydrogen generation is illustrated in figure 5. Pure TiO_2 nanoparticles have a negligible effect on the photocatalytic hydrogen generation rate, and similarly, pure Cu_2O nanomaterials have a negligible effect, but more catalytic activity than pure TiO_2 nanomaterials. TiO_2 Ag nanomaterials have seen a tenfold increase in their hydrogen generation rates after successful loading of Ag nanoparticles. The superior performance of TiO_2 Ag@Cu_2O nanocomposites in photocatalytic hydrogen synthesis compared to the other three systems demonstrates the many benefits of using a Z-type catalyst in photocatalytic hydrogen decomposition.

Conclusions

Comprehensive experiments on the issue of nanomaterials and autonomous processing technologies are described here. In this work, the multi-step oxidation procedure was used to successfully prepared three colloidal suspensions of graphene oxide (GO-1, 2, and 3) with various sheet sizes. Subsequently, three different sized go nanoflakes were investigated for their cellular biological effects. As expected, the data demonstrate that graphene oxide's cytotoxicity decreases with decreasing size. Furthermore, the absorption of graphene oxide by cells of varying sizes was studied. Graphene oxide cell absorption was shown to be size dependent, with the smallest size (Go-3) showing the maximum uptake.

In this study, using the attractor propagation (AP) clustering algorithm as a means of defect identification in wood was suggested. Since the quantity of AP clusters is sensitive to the chosen threshold P, the enhanced technique suggests automatically updating p value to ensure optimal clustering. Production planning, production operations, production tasks, and production execution are the several levels of the multi-tiered automatic production system proposed by the authors. Production goals are defined at the production plan layer, where they are broken down into concurrent production

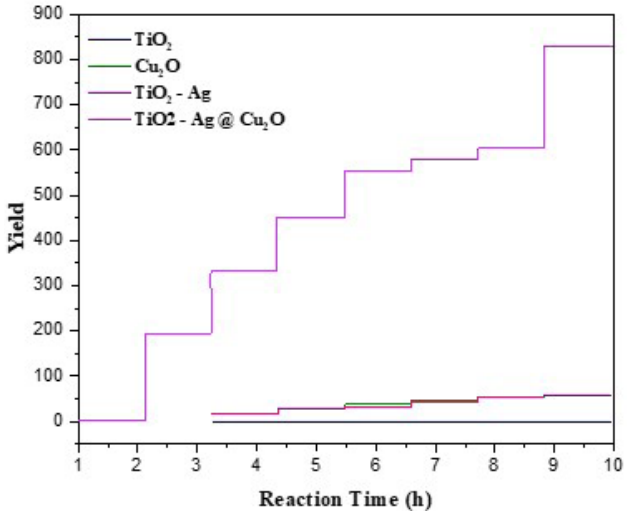

Figure 5: The effectiveness of four different materials in hydrogen photocatalysis.

jobs and subsequent production instances are created and handed off to the production execution layer. To facilitate the manufacturing of more extensive parametric goods for remote sensing, an autonomous production system makes use of an ontology database to lessen the limitations between production jobs and guarantee high concurrency.

The study's overarching goal is to make a precise evaluation of the controller's effect and to fine-tune its configuration and design as required. We have made great strides toward this goal by creating an electronic and electrical control system prototype for the vehicle. The physical layer network test was conducted for the new instrument table that has been produced as part of this project. To provide a thorough test report, it was necessary to create extensive test specifications and use cases. Our plan is to use this planned network testing method to provide the expected results. Several parts, including the power supply, oscilloscope, network monitoring, and industrial computer, have been prioritized in this effort. Our method entails completing the testing phase after integrating the test system, creating the testing procedure, setting up the test management software, and running the tests.

Acknowledgements

None.

Conflict of Interest

None.

References

1. Prasanth IS, Jeevanandam P, Selvaraju P, Sathish K, Hasane Ahammad SK, et al. 2023. Study of friction and wear behavior of graphene-reinforced AA7075 nanocomposites by machine learning. *J Nanomater* 2023: 1-15. https://doi.org/10.1155/2023/5723730
2. Kumar DD, Balamurugan A, Suresh KC, Kumar RS, Jayanthi N, et al. 2023. Study of microstructure and wear resistance of AA5052/B4C nanocomposites as a function of volume fraction reinforcement to particle size ratio by ANN. *J Chem* 2023: 1-12. https://doi.org/10.1155/2023/2554098

3. Girimurugan R, Selvaraju P, Jeevanandam P, Vadivukarassi M, Subhashini S, et al. 2023. Application of deep learning to the prediction of solar irradiance through missing data. *Int J Photoenergy* 2023: 1-17. https://doi.org/10.1155/2023/4717110
4. Baradaran S, Moghaddam E, Basirun WJ, Mehrali M, Sookhakian M, et al. 2014. Mechanical properties and biomedical applications of a nanotube hydroxyapatite-reduced graphene oxide composite. *Carbon* 69: 32-45. https://doi.org/10.1016/j.carbon.2013.11.054
5. Wahid MH, Eroglu E, LaVars SM, Newton K, Gibson CT, et al. 2015. Microencapsulation of bacterial strains in graphene oxide nano-sheets using vortex fluidics. *RSC Adv* 5(47): 37424-37430. https://doi.org/10.1039/C5RA04415D
6. Thiyagarajulu N, Arumugam S. 2021. Green synthesis of reduced graphene oxide nanosheets using leaf extract of *Lantana camara* and its *in-vitro* biological activities. *J Cluster Sci* 32(3): 559-568. https://doi.org/10.1007/s10876-020-01814-7
7. Ramesh AM, Kodandaram A, Swamy CK, Gangadhar A, Nagabhushana CM, et al. 2022. Fabrication of spherical porous pAg_2O-nWO_3/Ag/GNS heterostructure with enhanced photocatalytic activity through plasmonic S-scheme mechanism and its complementing biological interest. *Chemosphere* 294: 133715. https://doi.org/10.1016/j.chemosphere.2022.133715
8. Satishkumar P, Mahesh G, Meenakshi R, Vijayan SN. 2021. Tribological characteristics of powder metallurgy processed Cu-WC/SiC metal matrix composites. *Mater Today Proc* 37: 459-465. https://doi.org/10.1016/j.matpr.2020.05.449
9. Elsheikh AH, Shanmugan S, Muthuramalingam T, Thakur AK, Essa FA, et al. 2022. A comprehensive review on residual stresses in turning. *Adv Manuf* 1-26. https://doi.org/10.1007/s40436-021-00371-0
10. Satyanarayana G, Narayana KL, Rao BN. 2021. Incorporation of Taguchi approach with CFD simulations on laser welding of spacer grid fuel rod assembly. *Mater Sci Eng* 269: 115182. https://doi.org/10.1016/j.mseb.2021.115182
11. Satishkumar P, Krishnan GG, Seenivasan S, Rajarathnam P. 2023. A study on tribological evaluation of hybrid aluminium metal matrix for thermal application. *Mater Today Proc* 81: 1097-1104. https://doi.org/10.1016/j.matpr.2021.04.389
12. Biswas K. 2022. Ultrsonication mediated Iron-doped reduced graphene oxide nano-sheets exhibiting unique physico-chemical properties and biomedical applications. *Mater Chem Phys* 291: 126687. https://doi.org/10.1016/j.matchemphys.2022.126687
13. Satishkumar P, Rakesh AI, Meenakshi R, Murthi CS. 2021. Characterization, mechanical and wear properties of Al6061/Sicp/fly ashp composites by stir casting technique. *Mater Today Proc* 37: 2687-2694. https://doi.org/10.1016/j.matpr.2020.08.530
14. Dharmaiah G, Sridhar W, Balamurugan KS, Chandra Kala K. 2022. Hall and ion slip impact on magneto-titanium alloy nanoliquid with diffusion thermo and radiation absorption. *Int J Ambient Energy* 43(1): 3507-3517. https://doi.org/10.1080/01430750.2020.1831597
15. Wang X, Lu P, Li Y, Xiao H, Liu X. 2016. Antibacterial activities and mechanisms of fluorinated graphene and guanidine-modified graphene. *RSC Adv* 6(11): 8763-8772. https://doi.org/10.1039/C5RA28030C
16. Ghanem AF, Badawy AA, Mohram ME, Rehim MH. 2020. Synergistic effect of zinc oxide nanorods on the photocatalytic performance and the biological activity of graphene nano sheets. *Heliyon* 6(2). https://doi.org/10.1016/j.heliyon.2020.e03283
17. Abushanab WS, Moustafa EB, Harish M, Shanmugan S, Elsheikh AH. 2022. Experimental investigation on surface characteristics of Ti6Al4V alloy during abrasive water jet machining process. *Alex Eng J* 61(10): 7529-7539. https://doi.org/10.1016/j.aej.2022.01.004
18. He L, Dumée LF, Feng C, Velleman L, Reis R, et al. 2015. Promoted water transport across graphene oxide–poly (amide) thin film composite membranes and their antibacterial activity. *Desalination* 365: 126-135. https://doi.org/10.1016/j.desal.2015.02.032
19. Sharma A, Varshney M, Nanda SS, Shin HJ, Kim N, et al. 2018. Structural, electronic structure and antibacterial properties of graphene-oxide nano-sheets. *Chem Phys Lett* 698: 85-92. https://doi.org/10.1016/j.cplett.2018.03.010
20. Maleki N, Kashanian S, Nazari M, Shahabadi N. 2019. A novel and enhanced membrane-free performance of glucose/O_2 biofuel cell, integrated with biocompatible laccase nanoflower biocathode and glucose dehydrogenase bioanode. *IEEE Sens J* 19(24): 11988-11994. https://doi.org/10.1109/JSEN.2019.2937814
21. Askari N, Askari MB, Di Bartolomeo A. 2022. Electrochemical alcohol oxidation and biological properties of Mn_3O_4-Co_3O_4-rGO. *J Electrochem Soc* 169(10): 106511. https://doi.org/10.1149/1945-7111/ac96b2
22. Winkler DA. Chapter 9: Machine Learning at the (Nano)materials-biology Interface. In RSC Theoretical and Computational Chemistry Series. pp 206–226.
23. Grünewald F, Alessandri R, Kroon PC, Monticelli L, Souza PC, et al. 2022. Polyply: a python suite for facilitating simulations of macromolecules and nanomaterials. *Nat Commun* 13(1): 68. https://doi.org/10.1038/s41467-021-27627-4
24. Lee KZ, Basnayake Pussepitiyalage V, Lee YH, Loesch-Fries LS, Harris MT, et al. 2021. Engineering tobacco mosaic virus and its virus-like-particles for synthesis of biotemplated nanomaterials. *Biotechnol J* 16(4): 2000311. https://doi.org/10.1002/biot.202000311
25. Yu T, Su S, Hu J, Zhang J, Xianyu Y. 2022. A new strategy for microbial taxonomic identification through micro-biosynthetic gold nanoparticles and machine learning. *Adv Mater* 34(11): 2109365. https://doi.org/10.1002/adma.202109365
26. Li K, Sidorovskaia NA, Tiemann CO. 2020. Model-based unsupervised clustering for distinguishing Cuvier's and Gervais' beaked whales in acoustic data. *Ecol Inform* 58: 101094. https://doi.org/10.1016/j.ecoinf.2020.101094
27. Yao J, Jiang Z, Feng J, You R, Sun J, et al. 2021. Automatic processing technology based on nanomaterials. *Ferroelectrics* 579(1): 162-175. https://doi.org/10.1080/00150193.2021.1903255
28. Fernandes M, Pletl A, Thomas N, Rossi AP, Elser B. 2022. Generation and optimization of spectral cluster maps to enable data fusion of CaSSIS and CRISM Datasets. *Remote Sens* 14(11): 2524. https://doi.org/10.3390/rs14112524